

This article was downloaded by:

On: 23 January 2011

Access details: *Access Details: Free Access*

Publisher *Taylor & Francis*

Informa Ltd Registered in England and Wales Registered Number: 1072954 Registered office: Mortimer House, 37-41 Mortimer Street, London W1T 3JH, UK



## International Journal of Polymeric Materials

Publication details, including instructions for authors and subscription information:

<http://www.informaworld.com/smpp/title~content=t713647664>

## Ultra High Modulus Fibers from Solution and Melt Spinning

A. Ciferri<sup>a</sup>

<sup>a</sup> Istituto di Chimica Industriale, Università di Genova, Genoa, Italy

**To cite this Article** Ciferri, A.(1978) 'Ultra High Modulus Fibers from Solution and Melt Spinning', International Journal of Polymeric Materials, 6: 3, 137 – 158

**To link to this Article:** DOI: 10.1080/00914037808077905

**URL:** <http://dx.doi.org/10.1080/00914037808077905>

PLEASE SCROLL DOWN FOR ARTICLE

Full terms and conditions of use: <http://www.informaworld.com/terms-and-conditions-of-access.pdf>

This article may be used for research, teaching and private study purposes. Any substantial or systematic reproduction, re-distribution, re-selling, loan or sub-licensing, systematic supply or distribution in any form to anyone is expressly forbidden.

The publisher does not give any warranty express or implied or make any representation that the contents will be complete or accurate or up to date. The accuracy of any instructions, formulae and drug doses should be independently verified with primary sources. The publisher shall not be liable for any loss, actions, claims, proceedings, demand or costs or damages whatsoever or howsoever caused arising directly or indirectly in connection with or arising out of the use of this material.

# Ultra High Modulus Fibers from Solution and Melt Spinning†

A. CIFERRI

*Istituto di Chimica Industriale, Università di Genova, Genoa, Italy*

(Received June 28, 1977)

## I. INTRODUCTION

In recent years several methods for developing high strength–high modulus polymers have been reported. Restricting our consideration to the case of fibers, a general requirement for superior tensile properties appears to be a *high degree of extended chains and of molecular orientation along the fiber axis*. Various methods which have been used for developing ultra high modulus properties are summarized in Table I. The approach for maximizing chain extension and orientation differs depending whether the polymer molecule exhibits a flexible or a rigid conformation. In the case of flexible molecules, one

TABLE I  
 The ultra high modulus pursuit

Solid state deformations	} Flexible polymers
Polyethylene <sup>1</sup> $E_{11} \sim 700 \cdot 10^9$ dyne/cm <sup>2</sup> (Capaccio and Ward) ( $E_T \sim 2400 \cdot 10^9$ )	
Crystallization from strained solutions	
Polyethylene <sup>8</sup> $E_{11} \sim 1000 \cdot 10^9$ dyne/cm <sup>2</sup> (Pennings <i>et al.</i> )	} Rigid and semirigid polymers
Melt spinning	
Nylon 6 <sup>9</sup> $E_{11} \sim 150 \cdot 10^9$ dyne/cm <sup>2</sup> (Acierno <i>et al.</i> ) ( $E_T, \alpha \sim 1500 \cdot 10^9$ ) dyne/cm <sup>2</sup>	} Rigid and semirigid polymers
Solution spinning	
Kevlar 49 <sup>12</sup> $E_{11} \sim 1300 \cdot 10^9$ dyne/cm <sup>2</sup> ( $E_T \sim 1800 \cdot 10^9$ )	} Rigid and semirigid polymers
X-500 G <sup>15</sup> $E_{11} \sim 1000 \cdot 10^9$ dyne/cm <sup>2</sup>	
$E_{11}$ Steel $\sim 2000 \cdot 10^9$ dyne/cm <sup>2</sup>	

†Presented at the Gordon Conference on Fiber Science, New London, N.H., 1976.

seeks to *reduce* preformed chain folds, or *avoid* their formation, while simultaneously increasing the orientation. For samples crystallized under isotropic conditions this may be done by specialized cold drawing or extrusion processes, as reported by Capaccio and Ward,<sup>1</sup> by Porter and co-workers,<sup>2</sup> by Clark,<sup>3</sup> and by others.<sup>4,5</sup> The highest modulus thus obtained ( $E_{11}$ ) is already within a factor three from the theoretical modulus ( $E_T$ ). Alternatively, chain extension and orientation may be induced in a strain polymer solution, with the aid of a parallel velocity gradient, followed by crystallization of the oriented material. The approach has been discussed by Keller and co-workers in the case of polyethylene solutions flowing from opposed jets.<sup>6</sup> Recently, Penning and coworkers<sup>7,8</sup> have been able to grow continuous fibrillar polyethylene from seeded crystallization in a Couette apparatus. They reported the highest modulus so far attained for a polyethylene specimen. The case of melt spinning of flexible polymers<sup>9</sup> is also based on the maximization of chain extension and orientation in a strained melt, followed by crystallization of the oriented material.

A peculiar situation prevails in the case of rigid and semirigid polymers which have little tendency to fold and exhibit a natural tendency to form anisotropic solutions. In this case, the flow field may play a minor role, and the extension and orientation of the molecules is assisted by variables such as solvent type and polymer concentration. Since, due to their rigidity, these polymers have very high melting temperatures, solution spinning is the appropriate way to convert them into continuous fibers, as has been done by the Courtaulds,<sup>10</sup> the Monsanto,<sup>11</sup> and very successfully, by the du Pont Company.<sup>12</sup>

This paper is a critical review of the physical chemistry of the last two methods indicated in Table I, including our relevant results. The discussion begins with the method based on the solution spinning of rigid and semirigid molecules.

## II. SOLUTION SPINNING

### a) Theory

Figure 1 schematizes the formation of an oriented fiber from a solution of rigid rods. Intuitively, the formation of a fully oriented fiber is more easily achievable with the assistance of an oriented liquid phase (path 2) which may be regarded as an intermediate phase between random solution and pure parallelized polymer. In the case of real stiff molecules, such anisotropic solutions are experimentally observed and are also theoretically described. According to Flory,<sup>13</sup> the thermodynamic characteristics of anisotropic

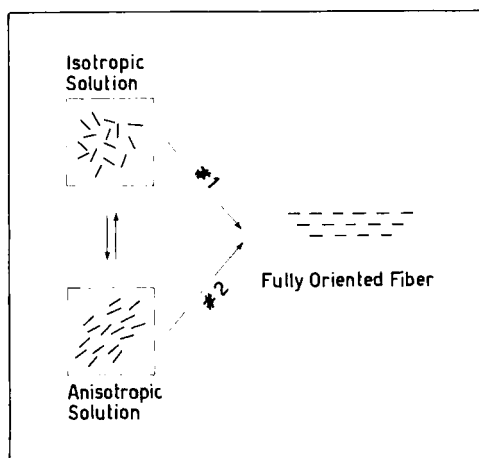


FIGURE 1 Schematic representation of solution spinning of rigid rods.

solution of rigid rods are described using the concept of *partial order*. Flory calculated the free energy of mixing pure solvent and pure parallelized polymer characterized by an asymmetry  $x$  (ratio length/diameter). The orientation of the axis of the rod, with respect to an orientation axis, was defined by a parameter  $y$  (disorientation parameter or orientation factor) which is equal to 1 in the case of perfect parallelization, and equal to  $x$  in the case of random solutions. The well known Flory's result is given by Eq. (1) which includes the numbers ( $n_1$  and  $n_2$ ) of solvent and polymer molecules, the corresponding volume fractions ( $v_1$  and  $v_2$ ), and the usual interaction parameter  $\chi_1$ . In the case of complete disorder ( $y = x$ ), Eq. (1) becomes similar to the familiar Flory-Huggins expression.<sup>14</sup> The equilibrium between the isotropic and anisotropic solutions is described<sup>13</sup> by equating the chemical potentials in the two phases, as indicated by Eqs. (2-5) (the prime denotes the anisotropic solution).

$$\Delta G_M/kT = n_1 \ln v_1 + n_2 \ln v_2 - (n_1 + yn_2) \ln [1 - v_2(1 - y/x)] + n_2 [\ln(xy^2) - y + 1] + \chi_1 xn_2 v_1 \quad (1)$$

$$\mu_1 = \mu'_1, \quad \mu_2 = \mu'_2 \quad (2)$$

$$\ln(1 - v_2) + \left(1 - \frac{1}{x}\right) v_2 + \chi_1 v_2^2 = \ln(1 - v'_2) + [(y - 1)/x] v'_2 + 2/y + \chi_1 v'_2{}^2 \quad (3)$$

$$\ln(v_2/x) + (x - 1)v_2 - \ln x^2 + \chi_1 x(1 - v_2)^2 = \ln(v'_2/x) + (y - 1)v'_2 + 2 - \ln y^2 + \chi_1 x(1 - v'_2)^2 \quad (4)$$

$$v'_2 = [x/(x - y)] [1 - \exp(-2/y)] \quad (5)$$

The last equation gives the variation of the orientation parameter with polymer concentration in the anisotropic phase. Plots derived from these equations are illustrated in Figure 2. The large diagram<sup>13</sup> illustrates the composition of coexisting isotropic and anisotropic phases as a function of  $\chi_1$ , for an axial ratio of 100. We note a narrow biphasic region where coexisting isotropic and anisotropic phases have similar composition, and a wide biphasic region in which the anisotropic phase is always very concentrated and the isotropic phase is always very diluted. The transition from narrow to wide biphasic

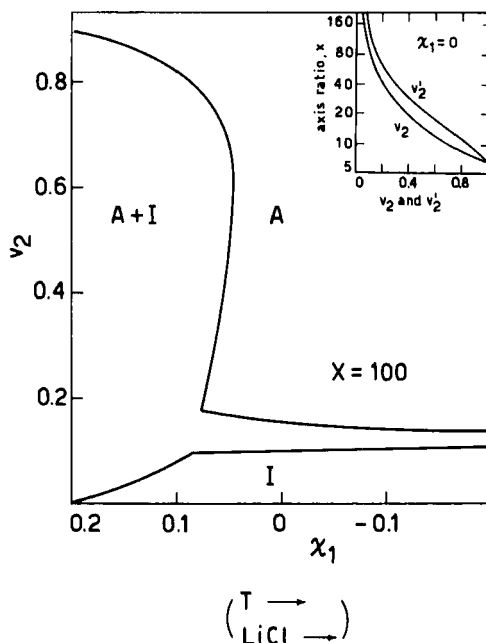


FIGURE 2 Composition  $v_2$  and  $v_2'$  of isotropic (I) and anisotropic (A) phases at equilibrium vs the interaction parameter  $\chi_1$  (and axis ratio) calculated by Flory. Reproduced from reference 13 by permission.

region occurs when the thermodynamic quality of the solvent is decreased ( $\chi_1 > 0$  indicates endothermal solutions). In the spinning process we are only interested in athermal or exothermal solvents for which the narrow biphasic region occurs. This because we cannot spin from the very concentrated solutions occurring with the poor solvents. Thus, it is appropriate to consider the narrow region in more detail. For  $v_2 < \sim 0.1$  only the isotropic phase is present, and for  $v_2 > \sim 0.15$  only the anisotropic solution exists. Since the

compositions within the narrow region are not affected by an increase of solvent power, an increase of temperature or of the concentration of a solubilizing agent such as LiCl (in cases in which they cause a decrease of  $\chi_1$ ), should be unsequential. A strong vertical displacement of the narrow biphasic region is however predicted if the degree of polymerization is altered. For instance, if  $x$  is reduced to 20, the isotropic phase is stable up to  $\sim 40\%$  polymer; while if  $x = 1000$ , the anisotropic phase is observed already in a  $\sim 1\%$  polymer solution. A simple relationship between the critical volume fraction for phase separation and axial ratio<sup>17</sup> is  $v_2^c \sim 8/x$ . It is also important to note the large effect of polymer concentration in increasing the orientation which is predicted by Eq. (5).  $y$  is already less than 10 when  $v_2 > \sim 0.2$ .

Flory's theory has been shown to be basically correct, and the predictions of this theory are very useful guidelines for the optimization of the mechanical properties of fibers produced by solution spinning. However, in order to make full use of this theory in connection with the spinning of anisotropic dopes, it is necessary to extend the treatment to account for some relevant complications. A summary of complicating factors includes the effects of: (1) a molecular weight distribution, (2) the possibility that the polymer-solvent interaction parameter, and the selective enrichment of a particular solvent component (i.e., LiCl), become phase-dependent, (3) partial flexibility, (4) liquid crystal  $\rightarrow$  crystal transformation, (5) elongational flow. We shall discuss in some detail the theoretical implications of partial flexibility, crystallization and elongational flow. Later, we shall analyze the experimental results. Concerning the first two topics, the effect of molecular weight distribution has not yet been systematically investigated. A fractionation effect during phase separation has been qualitatively observed by the du Pont scientists.<sup>16</sup> As expected, the higher molecular weight concentrated in the anisotropic phase. Recently, Flory<sup>17</sup> has extended his theory to polydisperse systems but the results have not yet been published. The second topics shall also not be considered in detail, essentially because the few data available are still insufficient for its proper evaluation.

A small degree of flexibility can be accounted for using Flory's treatment of semi-flexible polymers<sup>18</sup> which involves as a parameter the fraction,  $f$ , of bonds not in a colinear position. According to this treatment, if  $f$  is low enough and the molecular weight is great enough, the free energy of mixing pure solvent and ordered polymer may become positive. Under these conditions, the isotropic solution is no longer stable and phase separation occurs. No partial disorientation in the anisotropic phase is however considered in this theory. The phase equilibrium can be calculated using Eqs. (6)–(8).

$$\begin{aligned} \ln(1 - v_2) + (1 - 1/x)v_2 + \chi_1 v_2^2 = \\ = - \ln[1 + v_2'/x(1 - v_2')] + \chi_1 v_2'^2 \end{aligned} \quad (6)$$

$$\ln v_2 + (x-1)v_2 + (x-2)\ln(1-f) - \ln(Z/2) + x\chi_1(1-v_2)^2 = -\ln[x^{-1} + (1-v'_2)/v'_2] + \chi_1x(1-v'_2)^2 \quad (7)$$

$$f = 1/[1 + (Z-2)^{-1} \exp(E/RT)] \quad (8)$$

as done by Miller and coworkers<sup>19</sup> for different values of  $f$ . The shape of the calculated diagram is somewhat similar to that predicted by the rigid rod theory. However, on increasing flexibility, the narrow biphasic region is shifted to higher concentration and is also considerably widened. Miller and coworkers have attempted an interpretation of the phase diagram of poly- $\gamma$ -benzyl-L-glutamate in dimethylformamide using this theory. They were able to fit the experimental data on the basis of a variation of the fraction of non-linear bonds from 6 to 11%, corresponding to a temperature variation of 50°C. Alternatively, an approximate description of partial flexibility can be made in terms of a decrease of the "apparent" axial ratio using the rigid rod treatment as schematized in Figure 3(a). An increase of temperature, or LiCl concentration, is assumed to bring about a decrease of  $\chi_1$ , and of the dimensions of polymer molecules. While the effect of  $\chi_1$  would be unsequential, the decreased asymmetry ratio will push the narrow biphasic region toward higher polymer concentration. Should, at some critical temperature or LiCl concentration a helix  $\rightarrow$  coil type transition occur, an instability of the anisotropic solution will result. Additional calculations on the

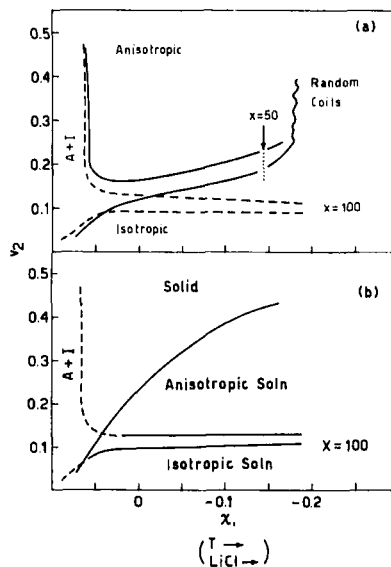


FIGURE 3 Schematic representation of the effect of partial flexibility (a) and of a liquid crystal  $\rightarrow$  crystal equilibrium (b) on the phase diagram of Figure 2.

flexibility problem have been recently made by Flory<sup>17</sup> and are, as yet, unpublished.

An additional complicating factor is illustrated in Figure 3(b). Flory's theory<sup>13</sup> is basically a phase separation theory based on entropy consideration of the most efficient way to arrange asymmetric molecules. Occurrence of forces acting among the particles is not required. A liquid crystal  $\rightarrow$  crystal transformation may however occur at some polymer concentration where *intermolecular forces* make the crystalline phase more stable than the liquid crystalline one. According to Flory's theory, essentially pure, ordered polymer should easily be observed in bad solvents. However, it is conceivable that even in good solvents, at some high enough polymer concentration, conventional crystallization can develop. In the case illustrated, the field of stability of the anisotropic solution is arbitrarily modified by a curve describing the liquid crystal  $\rightarrow$  crystal equilibrium. An increase of  $T$  or LiCl concentration is assumed to open up the field of stability of the liquid phase as usually observed. One should also be aware of the possible occurrence of *soluble* aggregated species, close to the precipitation line. These effects have been recently detected.<sup>20</sup>

Finally, the last factor relevant to fiber formation from anisotropic dopes is the modification of the phase diagram under the action of an extensional field. This effect is illustrated in the next figures. According to Marrucci,<sup>21</sup> under steady-state conditions, the orientation of rod-like molecules in an extensional flow is described by a contribution to the solution free energy given by Eq. (9).

$$\frac{\Delta G}{kT} = \frac{1}{2}Kn_2xy^2 \quad (9)$$

$$K = \frac{6}{8} \left( \frac{\Gamma l_1^2}{kT/\xi_1} \right) \simeq \Gamma 10^{-9} \quad (10)$$

$$\ln(1 - v_2) + \left( 1 - \frac{1}{x} \right) v_2 + \chi_1 v_2^2 = \ln(1 - v'_2) + [(y - 1)/x]v'_2 + 2/y + \chi_1 v'_2{}^2 - Kxy \quad (11)$$

$$\begin{aligned} \ln(v_2/x) + (x - 1)v_2 - \ln x^2 + \chi_1 x(1 - v_2)^2 + \frac{K}{2}x^3 = \\ = \ln(v'_2/x) + (y - 1)v'_2 + 2 - \ln y^2 + \chi_1 x(1 - v'_2)^2 - \frac{K}{2}xy^2 \end{aligned} \quad (12)$$

$$v'_2 = \frac{x}{x - y} \left[ 1 - \exp(-2/y + Kxy) \right] \quad (13)$$

The symbols have the usual meaning, and the constant  $K$  contains the parallel velocity gradient (or stretching rate)  $\Gamma$  (in  $\text{sec}^{-1}$ ), the dimension of an elementary segment of the rod  $l_1$  ( $\equiv$  rod length/ $x$ ), and the segmental diffusivity



given by the denominator of Eq. (10). The numerical constant depends only slightly upon the chosen model: the indicated value corresponds to the dumbbell model. A rough evaluation based on a  $l_1$  value in the order of  $10 \text{ \AA}$ , and on a monomer diffusivity in the order of  $10^{-5} \text{ cm}^2/\text{sec}$ , gives the approximation indicated on Eq. (10) which relates directly  $K$  to the parallel velocity gradient. The phase equilibrium between isotropic and anisotropic solutions subjected to elongational flow is calculated, as before, by equating the chemical potentials [Eqs. (11)–(13)], after inclusion of the terms corresponding to Eq. (9). Equation (13) gives the variation of the orientation parameter with polymer concentration. The equation predicts that, provided  $K$  is greater than a critical value  $K_{\text{crit}}$  (which implies a  $\Gamma$  greater than a critical  $\Gamma_{\text{crit}}$ ), the isotropic solution can no longer be observed. Detailed plots are shown in Figures 4 and 5. The critical value of the stretching rate is plotted as a function of the axial ratio  $x$  in the insert of Figure 4. For instance, for  $x = 100$ ,  $\Gamma_{\text{crit}} = 2000 \text{ sec}^{-1}$ . When  $\Gamma > 2000 \text{ sec}^{-1}$  the solution is anisotropic in the whole concentration range. When  $\Gamma < 2000 \text{ sec}^{-1}$  the anisotropic and isotropic phases may coexist. However, the compositions of the narrow biphasic region, which for the solution *at rest* are indicated by the value at  $\Gamma = 0$  on the

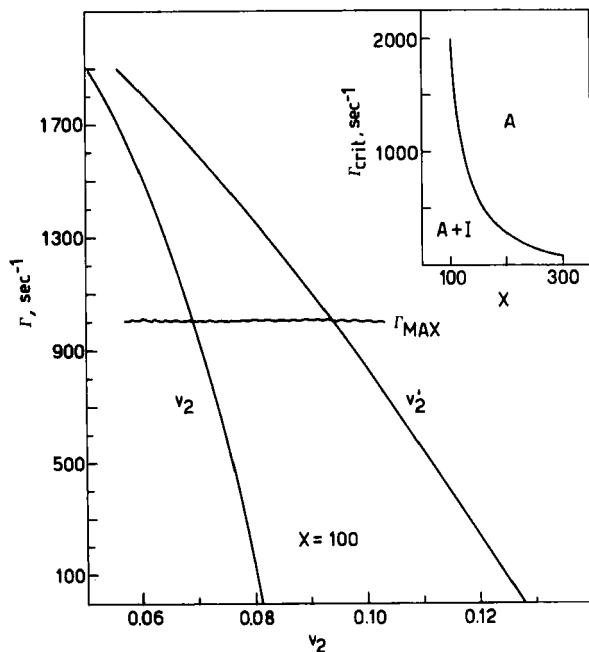


FIGURE 4 Effect of the parallel velocity gradient  $\Gamma$  on the composition of coexisting isotropic ( $v_2$ ) and anisotropic ( $v'_2$ ) phases. Cf. Text for insert. Data from reference 21.

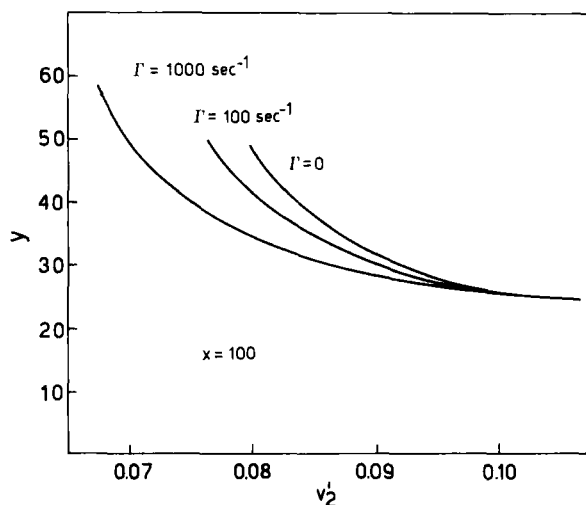


FIGURE 5 Flory's disorientation parameter as a function of polymer fraction for different values of the parallel velocity gradient. Data from reference 21.

large diagram, are shifted to lower polymer concentration on increasing the stretching rate.  $\Gamma_{MAX}$   $1000 \text{ sec}^{-1}$  is about the maximum value which may be practically reached. Altogether, the effect of the extensional flow appears to be a modest one. This is perhaps better evidenced by the plot (Figure 5) of the orientation parameter as a function of the gradient  $\Gamma$ . Only at low polymer concentration, the flow field is useful for increasing the orientation. However, if the polymer is soluble enough, it is always preferable to exploit the large orienting effect which is caused by an increase of polymer concentration. The elongational flow provides, of course, the direction of orientation along the continuous filament. Note, however, that in the case of semirigid chains the elongational field will play quite a significant role. Extension of the treatment to worm-like chains is in progress.

### b) Experimental behavior

We can now analyze the experimental behavior of two fiber forming polymers, poly-*p*-benzamide (PBA) and polyterephthalamide of *p*-aminobenzhydrazide (X-500) on the basis of the original theory and of the indicated complicating factors. The aim of the discussion is the selection of experimental conditions under which the mechanical properties of the fiber can be maximized. I should like to emphasize that most of our conclusions on PBA appears quite similar to those reached by the du Pont investigators in work which was performed independently, and certainly earlier than ours.

We first consider dilute solution data able to characterize the rigidity of high modulus polymers. Viscosity and light scattering data for PBA in sulfuric acid<sup>22</sup> recently obtained in Strasbourg indicate that the exponent  $a$  of the viscosity-molecular weight relationship is greater than one and decreases with molecular weight—a behavior typical of semirigid chains. (A similar viscosity-M.W. dependence has been reported by the du Pont group<sup>20</sup>). Application of the worm-like model gives<sup>22</sup> a persistence length,  $q$ , of  $\simeq 400 \text{ \AA}$ , a value similar to that observed for chains such as DNA.<sup>23</sup> The meaning of a persistence length of this size can be appreciated using the parameters of the benzamide unit indicated in Table II. The persistence length corresponds to a rod of molecular weight (i.e.  $M_n$ )  $\sim 8000$ , and to an asymmetry ratio of about 80, adequate to give a critical volume fraction for phase separation of  $\sim 10\%$ . Since the sample used in our investigations (cf. seq.) had a  $M_w$  of about 10,500, we have actually worked with a solute conforming to the ideal rigid rod model. Our solution data in dimethylacetamide (DMAc)/LiCl (Figure 6a) cannot be readily interpreted in terms of the effect of LiCl on persistence length. In fact, the decrease of intrinsic viscosity with LiCl content includes a variation of aggregation with salt concentration ( $C_s$ ) which is currently under investigation using other techniques. The size and shape of the aggregated species is of

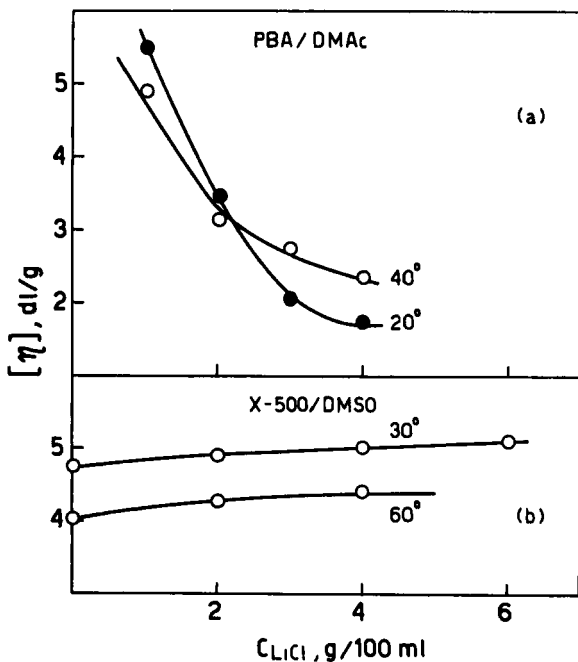
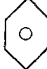


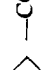





FIGURE 6 Variation of the intrinsic viscosity with LiCl concentration for PBA in DMAc (a), and for X-500 in DMSO (b) at different temperatures. Data from reference 28.

TABLE II  
Persistence length analysis for PBA and X-500  
(Data from reference 28)

	$\text{---CO---}$  $\text{---NH---}$  $\text{---NH---}$  $\text{---CO---NH---NH---CO---}$  $\text{---CO---}$ 	$5 \text{ \AA}$  $5 \text{ \AA}$	$15 \text{ \AA}$ 	$(\text{MW} = 119)$	$(\text{MW} = 281)$
$q$	400 Å			75 Å	
$n$ units	60			5	
Mol. weight	7250			1400	
$x$	80			15	
$\nu_2^c$	0.1			0.45	

considerable interest. Preliminary results obtained appear to indicate that at  $\sim 1\%$  LiCl the solute is nearly molecularly dispersed as a rod having an axial ratio of  $\sim 140$ . At  $\sim 4\%$  LiCl, however, there is already a considerable aggregation of PBA units, and a reduction of the axial ratio by about a factor 2 is observed. Occurrence of aggregation has also been indicated by the du Pont<sup>20</sup> and by Russian investigators.<sup>24</sup>

Also in the case of the X-500 molecule we are dealing with a semirigid chain as indicated by an exponent in the intrinsic viscosity–molecular weight relationship greater than one (as reported by Burke<sup>25</sup>). Our own intrinsic viscosity data in dimethylsulfoxide (DMSO)/LiCl, illustrated in Figure 6(b), reveal no aggregation, and allow an approximative evaluation of the persistence length using Ullman's theory<sup>26</sup> of the viscosity of worm-like chains. The result,  $q \simeq 75 \text{ \AA}$ , reveals a greater flexibility than in the case of PBA. The meaning of such a persistence length can be appreciated considering the parameters of the X-500 unit indicated in Table II. The persistence length corresponds to a rod of molecular weight (i.e.  $M_n$ )  $\sim 1400$ , and to an asymmetry ratio of 15, adequate to give a  $v_2^c$  of 45%. Since the molecular weight of our X-500 sample was 41,000, the chain contained several rod-like elements arranged in a worm-like manner.

Our results<sup>28</sup> for the viscosity-concentration behavior in concentrated solutions (determined with a Weissenberg rheogoniometer) are illustrated in Figure 7. The behavior of PBA is similar to that reported by other investigators.<sup>16,19,27</sup> The viscosity increases at first and then drops when, on increasing polymer concentration  $C_p$ , the low-viscosity anisotropic phase appears. When only the anisotropic phase is present the viscosity rises again with  $C_p$ . The maximum and the minimum are taken as the limit of the narrow biphasic region. At high shear stresses  $\tau$ , the viscosity is lower and the maximum and minimum tend to disappear. In the case of X-500 no maxima and minima are observed at low shear rate  $\dot{\gamma}$ , indicating that an anisotropic solution at rest is not formed. However, at high shear rate, the viscosity was found to decrease with time until it reached a plateau. The plateau values of  $\eta$ , plotted as a function of  $C_p$ , exhibit a maximum and a minimum. The effect needs additional investigation.

The extrapolation of the critical  $C_p$  values at zero shear stress yields data for the construction of the phase diagram for PBA<sup>29</sup> reported in Figure 8. The diagram includes a narrow biphasic region, a wide biphasic region, and a crystallization region. The latter two regions were determined using turbidimetric and analytical techniques. The peculiar shape of the diagram was quite unexpected and is somewhat different from that reported by others.<sup>19,30</sup> Since Flory's theory<sup>13</sup> deals with a two-component system, it is convenient to assume that each DMAc–LiCl mixture approximates a one-component diluent. The  $\chi_1$  value for a series of such diluents, differing only for the con-

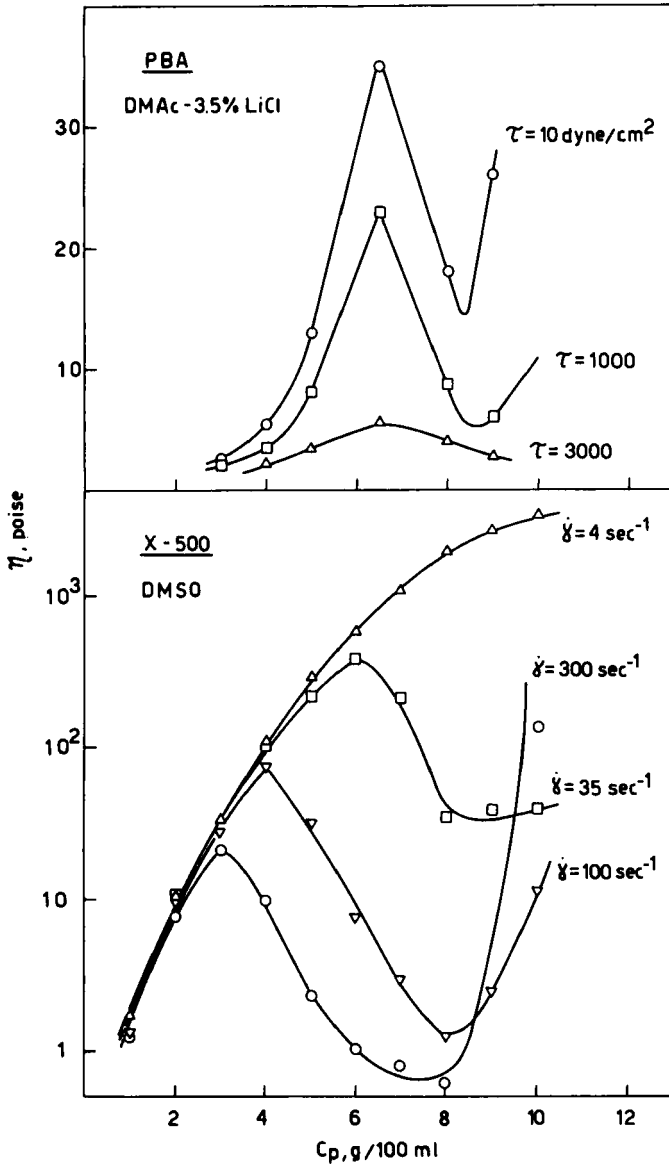


FIGURE 7 Variation of the viscosity of concentrated solutions with polymer concentration for PBA and X-500 at 20°C and for different values of shear stress,  $\tau$ , or shear rate,  $\dot{\gamma}$ . Data from reference 28.

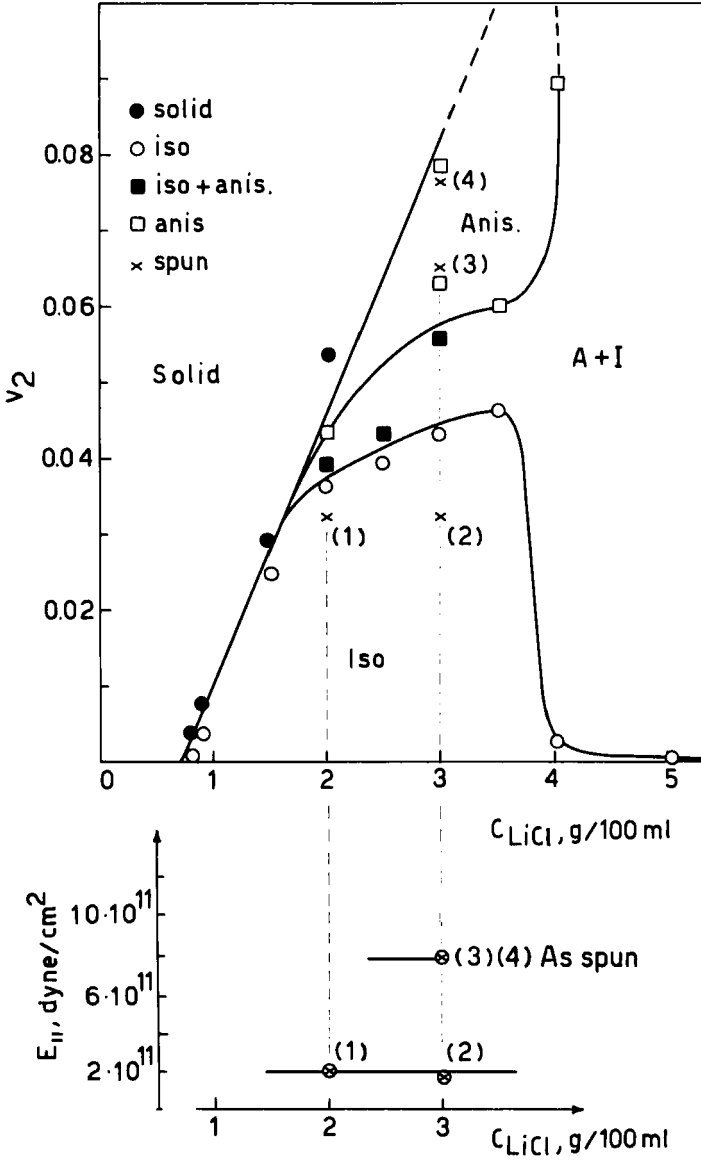


FIGURE 8 Phase diagram for PBA in DMAc/LiCl at 25°C. The initial modulus of fibers spun from the indicated solutions is reported on the lower part. Data from references 28 and 29.

centration of a salt of the LiCl type, has been shown to go *through a minimum on increasing  $C_s$*  in the case of several polymers systems.<sup>31,33</sup> This behavior is often referred to as a salting-in followed by a salting-out. It is reasonable to assume that this trend prevails also for the present system. On this basis, increased solvent power in the region of low salt concentration promotes the conventional solid  $\rightarrow$  liquid equilibrium even in the case in which the "liquid" is an anisotropic solution. Decreased solvent power on the right promotes the wide biphasic region predicted by Flory. We believe that the reason for which a wide biphasic region is observed only on the high salt concentration side is that salt binding reduces the interaction between PBA molecules or actually, between the soluble aggregates of PBA which—I recall—were evidenced by the dilute solution studies at high  $C_s$ . The narrow biphasic region is not parallel to the abscissa. In line with dilute solution results, this observation may be interpreted in terms of an increase of particle diameter resulting from aggregation. The critical polymer fraction, at low  $C_s$ , appears to be somewhat smaller ( $\sim 100\%$ ) than expected on the basis of the axial ratio calculated from the geometry of a single PBA molecule. Probably, the original theory underestimates the tendency to form anisotropic solutions when  $x$  is relatively small. A similar effect was noticed in earlier verifications of Flory's theory.<sup>13</sup> In any event, it is clear that by increasing LiCl content one is able to achieve: (1) *an increase of the solubility of PBA* and, (2) *a decrease of its apparent axial ratio*. We may ask if these alterations can be of advantage in connection with fiber spinning.

Solutions corresponding to the points indicated on the phase diagram were spun using adequate control of the various parameters affecting the spinning process. The corresponding modulus of "as spun" fibers<sup>28</sup> is projected on the lower part of the diagram. The modulus does not seem to be affected by aggregation or by alterations of flexibility caused by increasing  $C_s$ . The increased solubility caused by LiCl is however of significant advantage. In fact, the modulus greatly increases when the polymer concentration from which the fibers were spun is increased. This is attributed to the decrease of the disorientation factor  $\gamma$  with  $C_p$  which is predicted by the theory. As predicted, polymer concentration is truly the most important factor in solution spinning of rigid polymers. If one chooses a solvent in which  $C_p$  can be maximized (compatible with other factors affecting the spinning process), the solution can be almost completely oriented under equilibrium conditions and the elongational field brings negligible assistance to the orientation. This is essentially the high-point of the original discovery made by the du Pont group. Table III includes some earlier data taken from the du Pont patent which demonstrate the general improvement of mechanical properties due to the reduction of  $\gamma$  upon crossing the narrow biphasic region. Figure 9 represents our own data which substantiate the overall effect of polymer con-



TABLE III  
 Properties of as spun poly(*p*-benzamide) fibers  
 (Data from U.S. patent 3,671,542)

Source	Initial modulus $E_{11}$ , g/denier	Tensile strength $\sigma_b$ , g/denier	Elongation to break $\epsilon_b$ , percent	Orientation angle, deg
Isotropic layer	64	1.2	9.0	$\sim 40$
Anisotropic layer	283	7.2	8.1	$\sim 25$

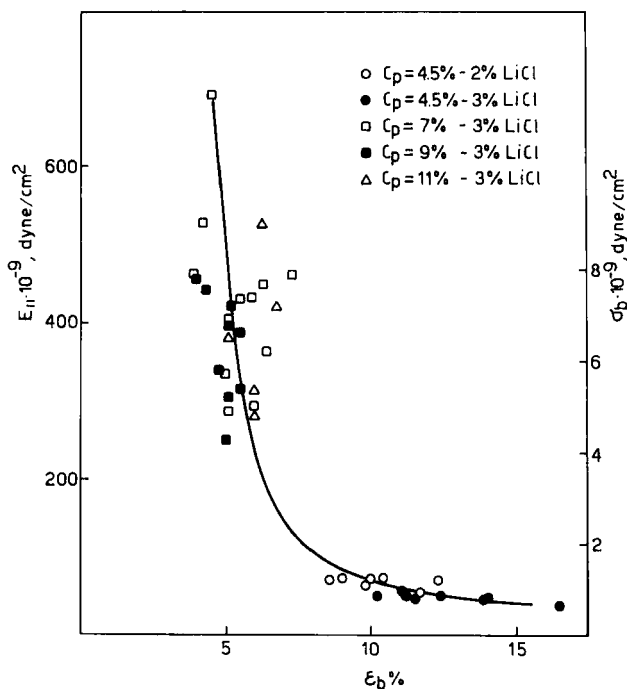


FIGURE 9 The modulus  $E_{11}$ , the tensile strength,  $\sigma_b$ , and the elongation to break,  $\epsilon_b$ , for fibers of PBA as spun from the indicated compositions. Data from reference 28.

centration on the modulus, the elongation to break, and the tensile strength. The increase of the modulus is always accompanied by a decrease of the elongation to break and an increase of tensile strength. The points are clustered according to the composition of dopes from which the fibers were spun.

The phase diagram for X-500<sup>34</sup> is reported in Figure 10. In this case rigidity seems insufficient to cause the occurrence of an anisotropic phase. The narrow biphasic region should theoretically appear somewhere between  $C_p \sim 5\%$  (on the basis of the axial ratio of the whole molecule) and  $C_p \sim 50\%$  (on the basis

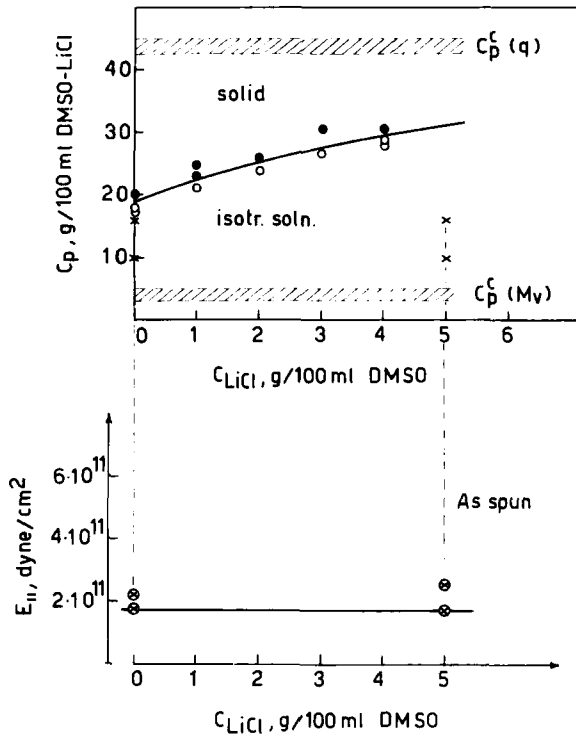


FIGURE 10 Solubility of X-500 in DMSO as a function of LiCl concentration.  $T = 25^\circ\text{C}$ . The initial modulus of fibers as spun from the indicated compositions is reported on the lower part. Data from references 28 and 34.

of the persistence length). Actually, the polymer can only crystallize from the isotropic solution when the saturation line is encountered on increasing  $C_p$ . Probably, the occurrence of crystallization prevents the attainment of high enough polymer concentration where the narrow region could be observed. X-500 fibers were spun from solutions corresponding to different points on the phase diagram. The modulus (projected on the lower part of the diagram) does not appear to be greatly affected by variations of salt concentration or of  $C_p$ , as was instead observed with PBA. In general, the most remarkable feature of X-500 is its ability to attain high modulus and orientation (comparable in some cases to that exhibited by PBA) in spite of its inability to form an anisotropic solution at rest. This finding indicates that spinning of anisotropic dopes in undoubtedly an elegant method, but certainly is not the only possible approach to superior mechanical performance from solution spinning. The likely interpretation of the X-500 behavior is that, for this semiflexible polymer, the elongational field provides the orientation which cannot be

provided at rest by an increase of  $C_p$ . (The relatively high molecular weight of X-500 may be particularly useful in this connection). In support of the latter interpretation, we note that we were able to increase the modulus of as spun X-500 fibers by increasing the pull-off (P.O.) ratio<sup>85</sup> during the spinning process. For instance, the modulus of about  $200 \cdot 10^9$  dynes/cm<sup>2</sup> reported in Figure 10 was obtained when P.O.  $\approx 1$ . When P.O.  $\approx 1.5$  the modulus was about  $500 \cdot 10^9$  dynes/cm<sup>2</sup>.

Although in a properly designed experiment perfect orientation could ideally be approached even for as spun fibers, in practice hot drawing is particularly convenient for improving the orientation and, hence, the modulus. This is illustrated in Figure 11 which is taken from the du Pont patent. The orientation angle is reduced to very low values as a result of the heat treatment, and, consequently, the modulus attain the 1000 g/den mark. Drawing is expected to be particularly useful in the case of X-500, but we have no experiments to substantiate this expectation.

### III. MELT SPINNING

The final part of this paper is concerned with melt spinning, and with the description of our method for increasing the elastic modulus of aliphatic

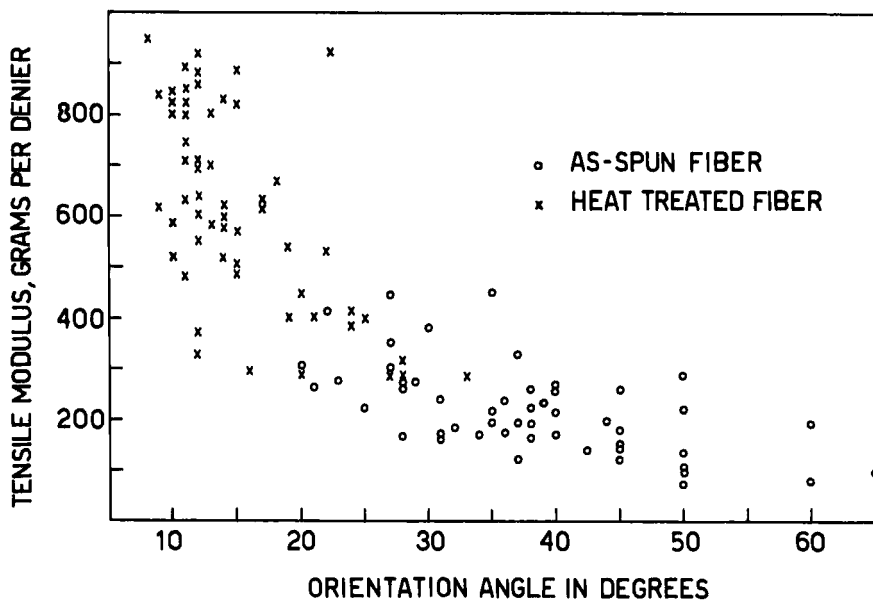


FIGURE 11 Reproduction of Figure 8 appearing in U.S. Patent 3,671,542 illustrating the effect of hot drawing on aromatic polyamide fibers.

polyamides. The rheological behavior of entangled systems, with particular regard to the role of the elongational flow, has not yet been amenable to satisfactory quantitative description. However, according to Marrucci,<sup>36</sup> a few qualitative considerations suggest that melt spinning—if properly exploited—should be a very useful tool for the production of highly oriented, high modulus fibers. These qualitative considerations are based on the theoretical analysis<sup>36</sup> on non-entangled systems (in particular low molecular weight melts). According to theory, two conditions must be fulfilled in order to achieve stretching and orientation of flexible molecules in extensional flow.<sup>36</sup> These conditions are illustrated by Eqs. (14) and (15).  $\Gamma$  is, again, the parallel velocity gradient and  $\lambda$  is the characteristic relaxation time of the material (largest relaxation time in Rouse's theory) under the conditions adopted.

$$\Gamma > \frac{0.5}{\lambda} \quad (14)$$

$$\Gamma t > \sim 4 \text{ (low M.W.)} \quad (15)$$

$$\text{draw ratio } S = \exp(\Gamma t) > \sim 50 \quad (16)$$

$$\lambda_{\text{Rouse}} = \frac{6\eta M}{\pi^2 \rho RT} \sim 10^{-5} \text{ sec (Nylon 6 } M < M_c) \quad (17)$$

According to Eq. (14),  $\Gamma$  must be large—when  $\lambda$  is small—in order to guarantee a *tendency* toward stretching and orientation. For *actual* stretching and alignment to occur, the stretching rate  $\Gamma$  has to be applied for a sufficient long period of time  $t$  necessary to completely stretch and orient the macromolecules. The product  $\Gamma t$  [Eq. (15)] must be greater than a value which is  $\sim 4$  for low molecular weight material, and increases with molecular weight. Thus, draw ratios [Eq. (16)] of  $\sim 50$  or higher are required, depending upon molecular weight. In the case of no entanglements ( $M < M_c$ ),  $\lambda$  calculated from Rouse theory [Eq. (17)] is in the order of  $10^{-5} - 10^{-4}$  sec which requires  $\Gamma$  values of  $10^4 - 10^5 \text{ sec}^{-1}$ , which cannot be attained in practice. Thus, there is no great tendency toward stretching and orientation.

Considering instead an entangled system, we may expect that

1) Since very large relaxation times are involved, small  $\Gamma$  values may be adequate for alignment. Moreover,

2) since the molecular weight of an entangled chain is relatively small ( $\sim M_c$ ), the time for alignment—hence the draw ratio—should be small.

We can indicate additional conditions apt to maximize the possibility of achieving alignment of flexible molecules during melt spinning. These may be the following ones:

- a) avoid high temperature leading to a reduction of  $\lambda$  in the initial part of the thread;
- b) prevent fast cooling and crystallization before orientation is maximized;
- c) select an entangled system in which slippage of junctions can occur but the number of junctions does not greatly decrease with deformation.

We believe that the nylon-salt systems which we have been investigating for several years<sup>37-40</sup> are just the right systems in which these conditions can be fulfilled. Data in Figure 12 illustrate<sup>39</sup> the effect of the addition of small quantities of LiCl or LiBr on the melt viscosity of nylon 6. The viscosity is greatly enhanced (even by a factor 10). The activation energy is not affected. There is only a vertical displacement suggesting that salts act as labile cross-linking agents. Data in Figure 13 illustrate<sup>38</sup> the strong effect of LiCl in

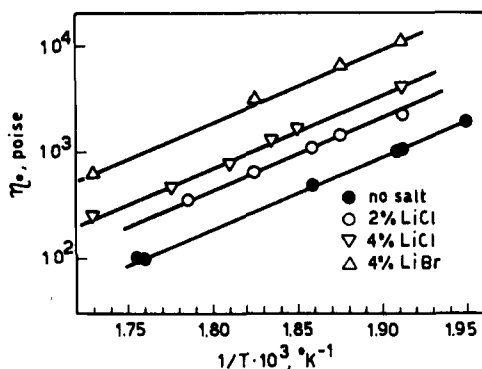


FIGURE 12 Zero shear melt viscosity vs reciprocal absolute temperature for nylon 6-salt systems. Data from reference 39.

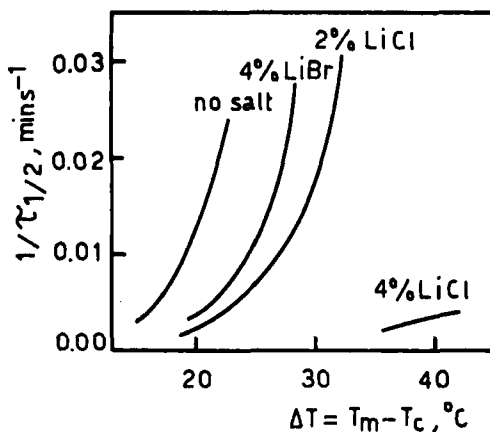


FIGURE 13 Reciprocal half-time of crystallization as a function of the difference between melting and crystallization temperature for nylon 6-salt systems. Data from reference 38.

depressing the crystallization rate of nylon 6. Under normal cooling conditions, it was, in fact, possible to prepare samples of salted nylon 6 with negligible crystallinity. However, under proper annealing conditions, the typical crystallinity of nylon 6 can be recovered.<sup>38</sup> Thus, this system may be significantly oriented in the amorphous state, thanks to the combined action of the salt in establishing crosslinkages, and in reducing crystallization rate. Results<sup>9</sup> for melt spun filaments of nylon 6-LiCl systems are exhibited in Table IV. The modulus of as spun samples is increased by LiCl. Independent X-ray data confirm that the nylon 6-LiCl samples are more oriented than the pure nylon 6 specimen. Annealing, performed in order to develop a maximum degree of crystallinity, confirms the higher modulus achieved by the salted samples. Drawing performed on as spun samples, and annealing of drawn samples, has negligible effect of pure nylon 6 but rises of about a factor 4 the modulus of salted samples. The real possibilities of the method are yet to be exploited. Work now in progress is directed toward an optimization of the conditions under which the salt helps to maximize the orientation.

TABLE IV  
The initial modulus of nylon 6-LiCl filaments  
(Data from reference 9)

Sample	$E_{11} \times 10^{-10}$ dynes/cm <sup>2</sup>			
	as spun	annealed	drawn	drawn and annealed
Ny 6	2.5	2.5	3.0	3.0
Ny 6-2% LiCl	2.0	3.8	9.0	11.0
Ny 6-4% LiCl	4.0	8.0	7.0	13.0

## References

1. G. Capaccio and I. M. Ward, *Polym. Eng. Sci.* **15**, 219 (1975).
2. R. S. Porter, J. H. Southern, and N. Weeks, *Polym. Eng. Sci.* **15**, 213 (1975).
3. E. S. Clark, *Polym. Prepr.*, Am. Chem. Soc., Div. Polym. Chem. **15**(1), 153 (1974).
4. T. Williams, *J. Mat. Sci.* **8**, 59 (1973).
5. K. Imada, T. Yamamoto, K. Shigematsu, and M. Takayanagi, *J. Mat. Sci.* **6**, 537 (1971).
6. M. R. Mackley and A. Keller, *Phil. Trans.*, Royal Soc. (London), **A278**, 29 (1975).
7. A. Zwijnenburg and A. J. Pennings, to be published in *Colloid and Polymer Science*.
8. A. Zwijnenburg and A. J. Pennings, *J. Polym. Sci.*, Polym. Letter Ed., **14**, 339 (1976).
9. D. Acierno, F. La Mantia, G. Polizzotti, G. Alfonso, and A. Ciferri, *J. Polym. Sci.*, Polym. Letter Ed., **6**, 323 (1977).
10. D. G. H. Ballard, J. D. Griffiths, and J. Watson, U.S. Pat. 3, 121, 766 (1964) assigned to Courtaulds, Ltd.
11. Symposium on High Modulus Aromatic Fibers, *J. Macrom. Chem.* **A7** (1973).
12. S. L. Kwolek, U.S. Pat. 3, 671, 542 (1972), assigned to the Du Pont Company.
13. P. J. Flory, *Proc. Roy. Soc. (London) Ser. A* **234**, 73 (1956).
14. P. J. Flory, *Principles of Polymer Chemistry*, Cornell Univ. Press, Ithaca, N.Y. (1953).
15. J. Preston, *Polym. Eng. Sci.* **15**, 199 (1975).

16. S. L. Kwolek, P. W. Morgan, J. R. Schaeffgen, and L. W. Gulrich, *Polym. Prepr., Am. Chem. Soc., Div. Polym. Chem.* **17(1)**, 53 (1976).
17. P. J. Flory, *Polym. Prepr., Am. Chem. Soc., Div. Polym. Chem.* **17(1)**, 46 (1976).
18. P. J. Flory, *Proc. Roy. Soc. (London) Ser. A* **234**, 60 (1956).
19. W. G. Miller, J. H. Ray, and E. L. Lee, *Liquid Crystals and Ordered Fluids* **2**, 243, R. Porter and J. Johnson, Eds., Plenum, New York (1974).
20. J. R. Schaeffgen, V. S. Foldi, F. M. Logullo, V. H. Good, L. W. Gulrich, and F. L. Killian, *Polym. Prepr., Am. Chem. Soc., Div. Polym. Chem.* **17(1)**, 69 (1976).
21. G. Marrucci and A. Ciferri, *J. Polym. Sci.*, (in press).
22. M. Arpin and C. Strazielle, *Makromol. Chem.* **177**, 581 (1976).
23. G. Bressan, R. Rampone, E. Bianchi, and A. Ciferri, *Biopolymers* **12**, 2227 (1974).
24. S. I. Banduryan, M. M. Iovleva, V. D. Kalmykova, S. P. Papkov, *Khim. Volokna* **5**, 73 (1975).
25. J. J. Burke, *J. Macromol. Sci.-Chem.* **A7(1)**, 187 (1973).
26. R. Ullman, *J. Chem. Phys.* **49**, 5486 (1968).
27. J. Hermans Jr., *J. Colloid Sci.* **17**, 638 (1962).
28. G. Alfonso, E. Bianchi, A. Ciferri, S. Russo, F. Salaris, and B. Valenti, *J. Polym. Sci., Part C*, (in press).
29. F. Salaris, B. Valenti, G. Costa, and A. Ciferri, *Makromol. Chem.* **177**, 3073 (1976).
30. M. Panar and L. F. Beste, *Polym. Prepr., Am. Chem. Soc., Div. Polym. Chem.* **17(1)**, 65 (1976).
31. L. V. Rajagh, D. Puett, and A. Ciferri, *Biopolymers* **3**, 421 (1965).
32. D. Puett and L. V. Rajagh, *J. Macromol. Chem.* **A2**, 111 (1968).
33. T. A. Orofino, A. Ciferri, and J. J. Hermans, *Biopolymers* **5**, 73 (1967).
34. A. Ciferri, *Polym. Eng. Sci.* **15**, 191 (1975).
35. A. Ziabicki, *Physical Fundamentals of Fiber Formation*, J. Wiley & Son Inc., New York (1976).
36. G. Marrucci, *Polym. Eng. Sci.* **15**, 229 (1975).
37. B. Valenti, G. Greppi, E. Bianchi, A. Tealdi, and A. Ciferri, *J. Phys. Chem.* **77**, 389 (1973).
38. E. Bianchi, A. Ciferri, A. Tealdi, R. Torre, and B. Valenti, *Macromolecules* **7**, 495 (1974).
39. D. Acierno, E. Bianchi, A. Ciferri, B. de Cindio, L. Nicolais, and C. Migliaresi, *J. Polym. Sci.* **C54** (1976).
40. B. Valenti, E. Bianchi, A. Tealdi, S. Russo, and A. Ciferri, *Macromolecules* **9**, 117 (1976).